

FSS-Based Smart Dataglove for Hand Gesture Recognition: Design and Implementation

Amanda M. D. Oliveira¹, João G. D. Oliveira², Valdemir P. Silva Neto¹ and Adaildo Gomes D'Assunção¹

¹ Departamento de Engenharia de Comunicações, UFRN Natal, RN, Brasil.

² Instituto Metr pole Digital

Abstract—This letter presents a fully textile band-stop frequency selective surface (FSS) designed to wearable technologies applications. The proposed structure features a center frequency of 3.6 GHz and a bandwidth of 150 MHz. It consists of two semicircles connected by a central conductive line and was prototyped using a conductive thread on a cotton textile dielectric. The structure was experimentally validated in the laboratory, analyzing its performance for angles of incidence and polarization ranging from 0° to 45°. Additionally, the FSS was integrated into a data glove to investigate its capability for gesture recognition. Variations in the S_{21} magnitude and phase at the resonance frequency were successfully correlated with distinct hand gestures, showcasing its potential for applications in human motion monitoring. The results, obtained through both simulation and experimental measurements, demonstrate the versatility and feasibility of the proposed structure for flexible and wearable applications. All findings are presented and thoroughly discussed in this study.

Index Terms—Embroidered structure, full textile, frequency selective surface, wearable technologies.

I. INTRODUCTION

FREQUENCY selective surfaces (FSS) are structures generally made up of periodic two-dimensional arrangements that act as spatial filters for electromagnetic waves propagating in free space. The behavior of these structures is determined by the elements of the arrangement, which can be designed to act as band-pass or band-reject filters. The choice between these modes of operation depends on the type of resonant element used, such as band-reject patches or band-pass apertures. These elements can be configured in different geometric shapes, according to the desired characteristics of the application [1].

FSSs have characteristics that make them a very relevant topic in the study of microwaves, among which we can mention the ease of implementation, the diversity of geometries and dimensions, and the large number of dielectric materials that can be used, which gives these structures wide applicability in the most diverse sectors: industrial, academic, commercial, and military [2]–[4].

When it comes to the type of dielectric substrate used in FSS designs, it is a widely used material in the literature to be mentioned. This is due to the ease with: 1) these materials can be found; 2) their main characteristics are consolidated and known; 3) they are easy to integrate with other components due to their characteristics.

At this point, it is understood that the most commonly used dielectrics are rigid dielectrics with single-layer printed circuit

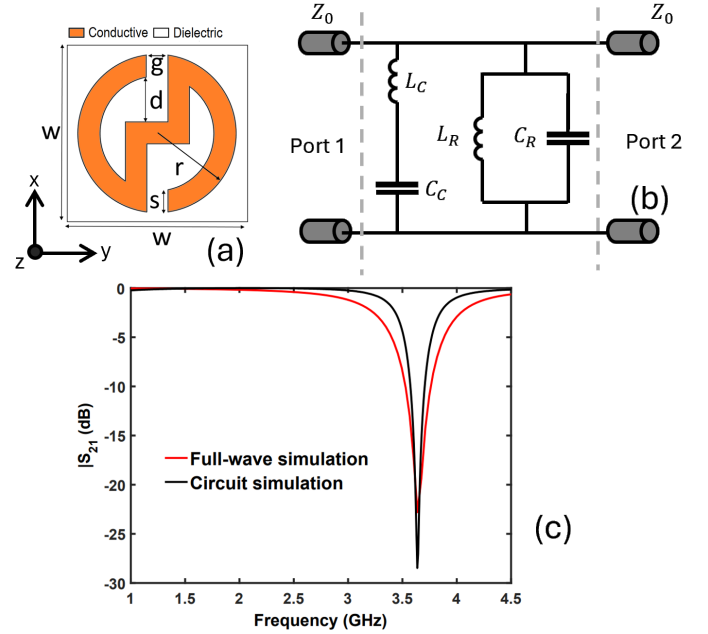


Fig. 1. Unit cell and its dimensions and simulated result for TE polarization.

boards, such as FR-4 epoxy fiberglass and various Rogers[®] dielectrics [5]–[7]. However, even within rigid dielectrics, it is possible to find studies using different materials as dielectrics, a good example being studies that use glass as a dielectric material [8]–[10]. However, these materials have the limitation that they cannot be used in applications that require greater flexibility or malleability. Flexible materials then emerged as a solution to the gap left by rigid materials.

We can relate the increase in their application to advances in technology, both in the materials industry and in manufacturing techniques. Among the applications that make use of this type of material, we can mention textile and wearable FSSs [11]–[13]. Although it is possible to develop FSS using flexible materials, by combining fabrics, plastic films, and flexible materials as substrates, along with deformation-resistant conductive materials [14]–[23]. Other materials can also be mentioned, but they are less commonly used because they have very specific characteristics. These include polymers such as silicone and polyethylene terephthalate (PET) [24] and F4B-2 [25].

One of the applications for which FSS have been used is the detection of gestures or hand movements within an

area. Systems that use wireless communication systems to detect gestures are becoming increasingly popular, especially as they offer an alternative to using cameras and have favorable characteristics for detecting small changes in the environment. These methods analyze the changes in the radio signal caused by the movement of the user's hands or body, and map the variations in amplitude and phase to identify different gestures, movements, or distances. Work such as [26] shows that these Wi-Fi-based systems can detect movement in large areas, even without a direct line of sight, opening up the possibility of applications in domestic and industrial environments [27]. These methods have shown promise for creating invisible and discreet interfaces where gesture detection is based solely on interference in the wireless signal, without invading the user's privacy.

In addition, motivated by the wide range of applications for these resources, researchers have dedicated themselves to the development of sensing techniques to detect movements with high precision. This technology can be implemented in areas such as security systems [28], sign language recognition [29], interfaces for digital games with virtual or augmented reality [30]–[32], and even in advanced robotics studies [33]. The versatility of these applications highlights the importance of exploring new approaches to gesture recognition in the search for interfaces that are increasingly intuitive and integrated into everyday life.

This letter presents the design and prototyping process of an FSS embroidered on cotton fabric. Unit cells have a circular topology with cuts that change the behavior of the structure at different angles of signal incidence. A fine conductive material, specifically a thread of silver fibers, the Shieldex 78f20, was used to prototype the FSS structure. The results indicate a bandwidth of 150 MHz. To analyze the behavior of the FSS at different angles of signal incidence, the structure was rotated from 0° to 45° . It was also placed on spherical surfaces with different radii. The process of designing the structure is described in detail in the next section, while the sections Materials Used and Experimental Results presents the prototyping process and the measured results. After analyzing the structure, it is used to identify different hand gestures.

II. UNIT CELL DESIGN AND EQUIVALENT CIRCUIT ANALYSIS

A. Unit Cell Geometry Evolution

Aiming to design an FSS that can be used in wearable devices, within the wireless technology, more specifically using sub-6GHz 5G operational band, in the center of the n78 band, which covers 3.4-3.8GHz, a unit cell in the shape of a circular ring was developed. The development and evolution of the geometry of the proposed FSS unit cell are presented in detail in Fig. 2.

The element exhibits a band-stop behavior, as shown in Fig. 2. The initial unit cell design (v1) comprised two unconnected semicircles, with an operating frequency above 10 GHz due to its small size. To lower this frequency, parallel arms were added in v2, but without connection, keeping the operating band above the desired range. Finally, a perpendicular element

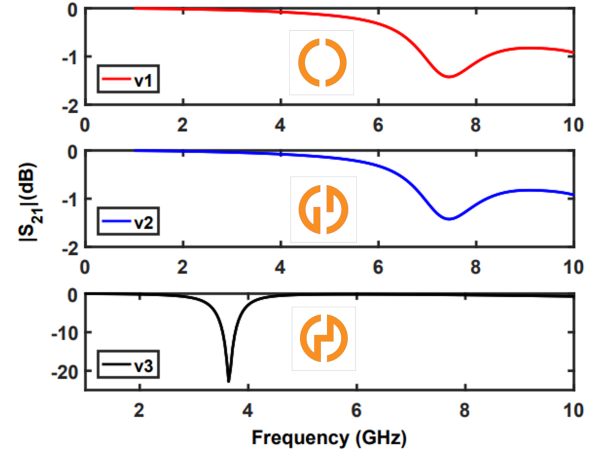


Fig. 2. Evolution of unit cell.

was introduced in v3, connecting the arms and increasing the electrical length, resulting in a resonance frequency of 3.6 GHz with a 300 MHz bandwidth. The asymmetrical geometry was chosen to align with specific application requirements, which will be detailed later.

All dimensions of the final unit cell are detailed in Fig. 1(a). In this work, simulations were conducted using two methods to validate the design: the full-wave method implemented in Ansys HFSS and the Equivalent Circuit Model (ECM) using Agilent Advanced Design System. An infinite array approximation and lumped elements were employed, based on the modeling characteristics of the unit cell, which has the following dimensions: $g = 2$ mm, $s = 2.02$ mm, $d = 4.4$ mm, $r = 7.5$ mm, and $W = 20$ mm.

B. Equivalent Circuit Model

The design of the equivalent circuit model (ECM) for the unit cell proposed in this work was simulated using Agilent Advanced Design System (ADS) software. The ECM of the element shown in Fig. 2 as model (v3) is illustrated in Fig. 1(b). The two semicircular elements can be modeled as a parallel LC resonator, where both elements contribute significantly to the inductance value. The element added to connect the two semicircles introduces a series LC element, which has a strong influence on the resonance frequency of the final design. The dielectric substrate used, a fabric made entirely of cotton, can be modeled as a transmission line. However, due to its very small thickness, the effect of this transmission line can be neglected in this modeling [34]. Table I shows the values of the ECM parameters of the proposed element.

The values of the parameters were obtained using the Ansys HFSS optimization tool, based on the transmission zero resonance equation presented in Eq. 1 [8].

$$f_z = \frac{1}{2\pi\sqrt{L_n C_n}}, n = R, C. \quad (1)$$

TABLE I
PARAMETERS OF CIRCUIT MODEL

L_R	C_R	L_C	C_C
15nH	0.1pF	12.5nH	0.15pF

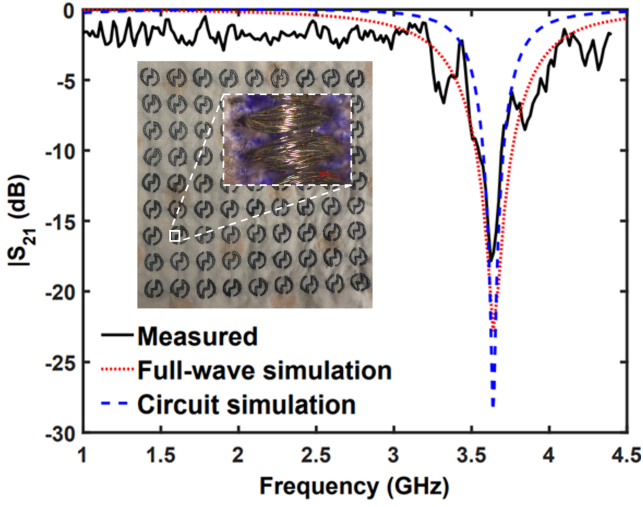


Fig. 3. Comparison between simulated and measured results for the constructed prototype.

III. EMPLOYED MATERIALS

A. Dielectric Materials

In this work, a commercial fabric made from 100% cotton threads was used as the dielectric material of the FSS, both for the weft and warp. The thickness of the cotton thread is 0.2 mm, and the cotton used was of type 72f20, indicating that the fabric employed has 72 filaments with 20 dtex.

Fig. 3 illustrates that the fabric used contains gaps in its structure, which affects the effective permittivity (ϵ_{eff}) by reducing the influence of the dielectric properties of the material on the conductive element. In this study, the dielectric material was characterized with values of $\epsilon_{eff} = 1.5$ e $\delta = 0.0032$. This fabric was selected due to its excellent malleability and ease of use during the manufacturing process.

B. Conductive Materials

In this work, a silver conductive thread was used as the conductive material, specifically the Shieldex® 78/20 thread and has a titre of 78dtex and a round cross-section. This thread is composed of fiber yarns and conductive yarns. The material is polyamid/nylon 6 and the electrical resistivity is about $3.5k\Omega/m$ [35].

IV. EXPERIMENTAL RESULTS

For validation of the previously described project, an FSS was prototyped and measured using the free-space method. The FSS was a matrix structure of unit cells with dimensions of 9x9. Prototyping this structure involved four steps: 1) Computerized printing of the matrix on adhesive sheets; 2) Transfer of the adhesive onto fabric to mark the unit cells; 3) Marking the unit cells on the cotton fabric following

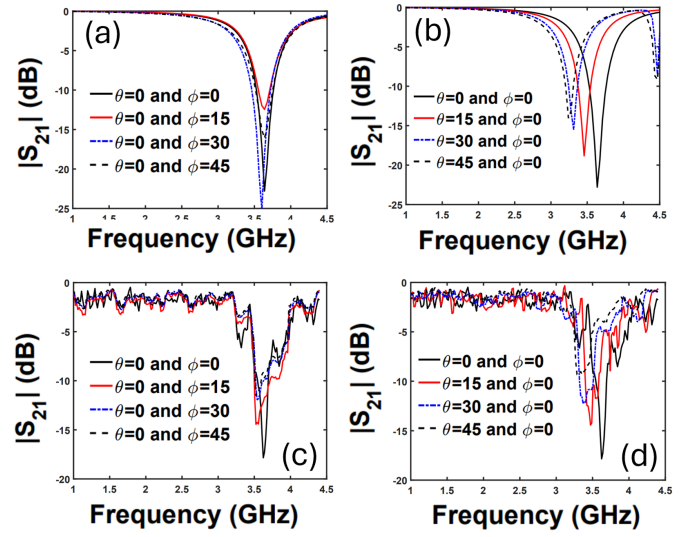


Fig. 4. Measured results of the FSS: (a) Simulated angle of incidence; (b) Simulated angle of polarization; (c) Measured angle of incidence; (d) Measured angle of polarization.

the adhesive guide; 4) Placing (hand-made embroidery) the conductive material to fill the unit cells with the conductive material. Fig. 3 presents the builded and measured prototype, with a zoomed-in view highlighting the detailed filling of each unit cell.

As can be observed in Fig. 3, each cell of the developed structure was fully filled using embroidery. Fig. 3 presents the measured results of the FSS for TE polarization, which is the polarization mode of interest due to its single well-defined resonance. This can be considered a key factor in certain applications based on the operating band of the structure. Therefore, all analyses, such as changes in polarization and incidence angle, will be conducted around the TE mode.

A. Obtained results

This section presents experimental results obtained from prototyping a full-textile FSS with conductive threads embroidered into the dielectric. Fig. 3 shows the results obtained from measuring the FSS in TE polarization with normal incidence to the z-axis of the structure. Based on the result illustrated in Fig. 3 and 5, it is noteworthy that the FSS exhibited a response close to the simulated result, with the operating frequency centered at 3.6 GHz. This can be attributed to the conformal nature of embroidering the thread into the fabric used as dielectric.

Being a commercial material, the conductive characteristics of the thread, coupled with its ease of implementation, favor prototyping, and the obtained results demonstrate high fidelity to the simulated design. Fig. 4 depict the measured results from varying the incidence angle and polarization of the prototyped FSS.

As observed in Fig. 4(c) and Fig. 4(d), the measured results for different angles showed behaviors similar to those simulated in Fig. 4(a) and Fig. 4(b). Regarding polarization change, there is a shift in the rejection band of the FSS,

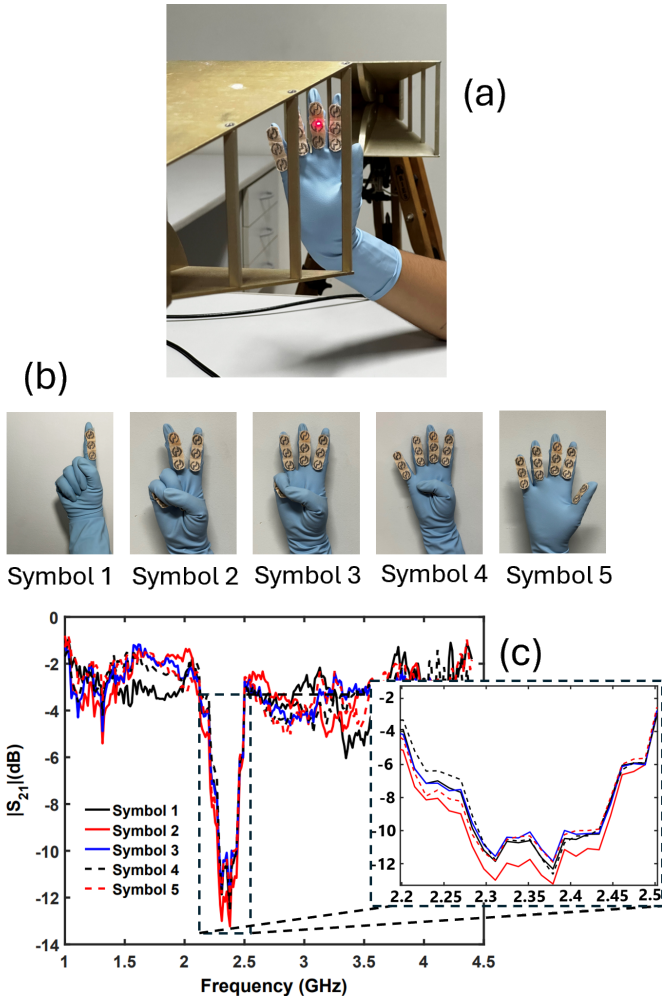


Fig. 5. FSS applied to hand gesture recognition: (a) Measurement setup; (b) Symbols measured; (c) Result obtained from data glove measurement.

whereas, for the change in incidence angle, only a variation in the S_{21} magnitude is noticeable.

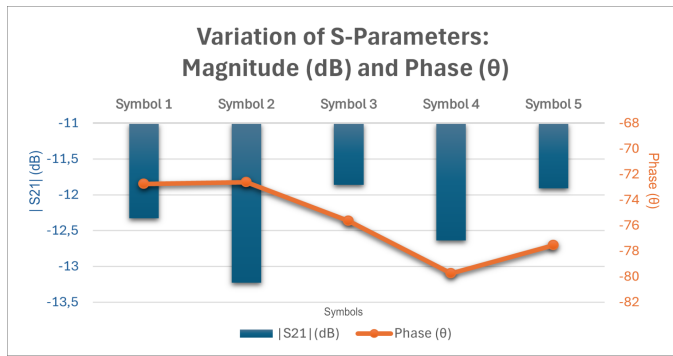


Fig. 6. Results obtained from analysis of the data glove measurements.

V. APPLICATION: HAND GESTURE RECOGNITION

Based on the experimental results presented in the previous sections, we can conclude that the proposed device exhibits angular and incidence instability characteristics that may be advantageous for gesture recognition. To evaluate this, the

proposed FSS was integrated into a rubber glove, and measurements were conducted for different hand gestures. The measured results are shown in Fig. 5. It shows the structure having different frequency responses, even though all are centered around 2.35 dB when the gestures are changed.

With the results obtained from measuring the S parameters of the proposed data glove, it was possible to identify the variation in both the modulus S_{21} and the corresponding phase in the element's resonance frequency. These results, shown in Fig. 6, demonstrate the sensitivity of the device to different gesture configurations, highlighting its potential for applications in motion recognition.

VI. CONCLUSION

In this letter, a new structure was presented and investigated. The flexible textile structure was designed, prototyped, and subjected to experimental validation, using 100% cotton fabric as the dielectric material. A flexible material was employed as a conductor: a thread composed of silver fibers. The results, obtained through simulation and experimental measurements, indicate significant potential for the application of these structures in wearable technologies. This potential stems from the intrinsic characteristics of these structures, which exhibit limited stability with respect to both the angle of incidence and the polarization angle. In addition, the structure was integrated into a data glove and evaluated for its ability to recognize different hand gestures. The measurements showed that variations in the S_{21} magnitude and phase at the resonance frequency corresponded to distinct manual gestures. This highlights the structure's feasibility for gesture recognition applications, making it suitable for use in devices that monitor human motion or detect changes in position. These results validate the deformation-resistant materials used and confirm their potential for innovative wearable applications.

REFERENCES

- [1] M. J. Duarte, V. P. d. Silva Neto, and A. G. D'Assunção, "A new miniaturized low-profile and stable dual-band fss with 2.5 d structure for ism bands," *Journal of Microwaves, Optoelectronics and Electromagnetic Applications*, vol. 21, pp. 445–452, 2022.
- [2] P. Wang, W. Jiang, T. Hong, Y. Li, G. F. Pedersen, and M. Shen, "A 3-d wide passband frequency selective surface with sharp roll-off sidebands and angular stability," *IEEE Antennas and Wireless Propagation Letters*, vol. 21, no. 2, pp. 252–256, 2021.
- [3] B. Wu, D. Zhang, B. Chen, Y.-J. Yang, Y.-T. Zhao, and T. Su, "Broadband low-profile frequency selective absorber using ultraminiaturized metal-graphene structure," *IEEE Antennas and Wireless Propagation Letters*, vol. 21, no. 12, pp. 2422–2426, 2022.
- [4] N. Kou and S. Yu, "Angular selectivity based on odd mode resonance of frequency selective surface," *IEEE Antennas and Wireless Propagation Letters*, vol. 21, no. 11, pp. 2151–2155, 2022.
- [5] R. Fardel, M. Nagel, F. Nüesch, T. Lippert, and A. Wokaun, "Fabrication of organic light-emitting diode pixels by laser-assisted forward transfer," *Applied Physics Letters*, vol. 91, no. 6, 2007.
- [6] D. Comite and N. Pierdicca, "Decorrelation of the near-specular land scattering in bistatic radar systems," *IEEE Transactions on Geoscience and Remote Sensing*, vol. 60, pp. 1–13, 2021.
- [7] H. V. Habi and H. Messer, "Recurrent neural network for rain estimation using commercial microwave links," *IEEE Transactions on Geoscience and Remote Sensing*, vol. 59, no. 5, pp. 3672–3681, 2020.
- [8] H. Chen, H. Chen, X. Xiu, Q. Xue, and W. Che, "Transparent fss on glass window for signal selection of 5g millimeter-wave communication," *IEEE Antennas and Wireless Propagation Letters*, vol. 20, no. 12, pp. 2319–2323, 2021.

- [9] U. Farooq, M. F. Shafique, A. Iftikhar, and M. J. Mughal, "Polarization-insensitive triband fss for rf shielding at normal and higher temperatures by retrofitting on ordinary glass windows," *IEEE Transactions on Antennas and Propagation*, vol. 71, no. 4, pp. 3164–3171, 2023.
- [10] Z. Chen, Y. Li, Z. Wang, J. Hu, and X. Yao, "Energy-saving glass loading dual-band miniaturized fss for rf shielding with high oblique stability and optical transparency," *IEEE Transactions on Electromagnetic Compatibility*, 2024.
- [11] J. G. De Oliveira, A. M. Oliveira, M. D. Mesquita, V. P. Neto, and A. G. D'assunção, "Development of a textile device applied to hand gesture recognition," in *2023 SBMO/IEEE MTT-S International Microwave and Optoelectronics Conference (IMOC)*. IEEE, 2023, pp. 214–216.
- [12] S. Amit, V. Talasila, T. Ramya, and R. Shashidhar, "Frequency selective surface textile antenna for wearable applications," *Wireless Personal Communications*, vol. 132, no. 2, pp. 965–978, 2023.
- [13] B. Sugumaran, R. Balasubramanian, and S. K. Palaniswamy, "Performance evaluation of compact fss-integrated flexible monopole antenna for body area communication applications," *International Journal of Communication Systems*, vol. 35, no. 6, p. e5085, 2022.
- [14] M. Ghebrehirhan, F. Aranda, G. Walsh, D. Ziegler, S. Giardini, J. Carlson, B. Kimball, D. Steeves, Z. Xia, S. Yu *et al.*, "Textile frequency selective surface," *IEEE Microwave and Wireless Components Letters*, vol. 27, no. 11, pp. 989–991, 2017.
- [15] İ. Üner, S. Can, B. H. Gürcüm, A. E. Yılmaz, and E. Aksoy, "Comparative analysis of embroidery and screen-printing techniques for textile-based frequency selective surfaces," *Tekstil ve Mühendis*, vol. 30, no. 131, pp. 243–248, 2023.
- [16] M. M. Tahseen and A. A. Kishk, "Flexible and portable textile-reflectarray backed by frequency selective surface," *IEEE Antennas and Wireless Propagation Letters*, vol. 17, no. 1, pp. 46–49, 2017.
- [17] O. Rac-Rumijowska, P. Pokryszka, T. Rybicki, P. Suchorska-Woźniak, M. Woźniak, K. Kaczkowska, and I. Karbownik, "Influence of flexible and textile substrates on frequency-selective surfaces (fss)," *Sensors*, vol. 24, no. 5, p. 1704, 2024.
- [18] N. Naseer, D. Gokcen, and B. Saka, "Analysis and design of stopband fss unit cell on textile substrates," *IEEE Letters on Electromagnetic Compatibility Practice and Applications*, vol. 3, no. 1, pp. 15–18, 2020.
- [19] İ. Üner, S. Can, B. H. Gürcüm, A. E. Yılmaz, and E. Aksoy, "Design and implementation of a textile-based embroidered frequency selective surface," *Textile and Apparel*, vol. 32, no. 4, pp. 297–303, 2022.
- [20] W. Whittow, Y. Li, R. Torah, K. Yang, S. Beeby, and J. Tudor, "Printed frequency selective surfaces on textiles," *Electronics Letters*, vol. 50, no. 13, pp. 916–917, 2014.
- [21] H. Mirza and N. Sultana, "A wideband flexible electro-textiles material linear-to-circular polarizing metasurface for s-band cubesat," *Materials Today: Proceedings*, 2023.
- [22] M. D. S. Mesquita, A. G. D'Assunção, J. B. L. Oliveira, and Y. M. V. Batista, "A new conductive ink for microstrip antenna and bioinspired fss designs on glass and fiberglass substrates," *Journal of Microwaves, Optoelectronics and Electromagnetic Applications*, vol. 18, no. 2, pp. 227–245, 2019.
- [23] J. G. De Oliveira, A. M. Oliveira, M. D. Mesquita, V. P. Neto, and A. G. D'assunção, "Development of a textile device applied to hand gesture recognition," in *2023 SBMO/IEEE MTT-S International Microwave and Optoelectronics Conference (IMOC)*. IEEE, 2023, pp. 214–216.
- [24] O. Rac-Rumijowska, P. Pokryszka, T. Rybicki, P. Suchorska-Woźniak, M. Woźniak, K. Kaczkowska, and I. Karbownik, "Influence of flexible and textile substrates on frequency-selective surfaces (fss)," *Sensors*, vol. 24, no. 5, p. 1704, 2024.
- [25] H. Wang, L. Zheng, M. Yan, J. Wang, S. Qu, and R. Luo, "Design and analysis of miniaturized low profile and second-order multi-band polarization selective surface for multipath communication application," *IEEE Access*, vol. 7, pp. 13 455–13 467, 2019.
- [26] P. Hu, C. Tang, K. Yin, and X. Zhang, "Wigr: a practical wi-fi-based gesture recognition system with a lightweight few-shot network," *Applied Sciences*, vol. 11, no. 8, p. 3329, 2021.
- [27] Y. Gu, X. Zhang, Y. Wang, M. Wang, H. Yan, Y. Ji, Z. Liu, J. Li, and M. Dong, "Wigrunt: Wifi-enabled gesture recognition using dual-attention network," *IEEE transactions on human-machine systems*, vol. 52, no. 4, pp. 736–746, 2022.
- [28] N. Dhruva, S. R. Rupanagudi, and H. Neelkant Kashyap, "Novel algorithm for image processing based hand gesture recognition and its application in security," in *International Conference on Advances in Computing, Communication and Control*. Springer, 2013, pp. 537–547.
- [29] G. Monti, G. Porcino, and L. Tarricone, "Textile chipless tag for gesture recognition," *IEEE Sensors Journal*, vol. 21, no. 16, pp. 18 279–18 286, 2021.
- [30] F. Liu, B. Du, Q. Wang, Y. Wang, and W. Zeng, "Hand gesture recognition using kinect via deterministic learning," in *2017 29th Chinese Control and Decision Conference (CCDC)*. IEEE, 2017, pp. 2127–2132.
- [31] F. Liu, W. Zeng, C. Yuan, Q. Wang, and Y. Wang, "Kinect-based hand gesture recognition using trajectory information, hand motion dynamics and neural networks," *Artificial Intelligence Review*, vol. 52, pp. 563–583, 2019.
- [32] B. Hisham and A. Hamouda, "Supervised learning classifiers for arabic gestures recognition using kinect v2," *SN Applied Sciences*, vol. 1, no. 7, p. 768, 2019.
- [33] J. Pan, Y. Li, Y. Luo, X. Zhang, X. Wang, D. L. T. Wong, C.-H. Heng, C.-K. Tham, and A. V.-Y. Thean, "Hybrid-flexible bimodal sensing wearable glove system for complex hand gesture recognition," *ACS sensors*, vol. 6, no. 11, pp. 4156–4166, 2021.
- [34] M. Nauman, R. Saleem, A. K. Rashid, and M. F. Shafique, "A miniaturized flexible frequency selective surface for x-band applications," *IEEE Transactions on Electromagnetic Compatibility*, vol. 58, no. 2, pp. 419–428, 2016.
- [35] "Shieldex® 78/20 — shieldex.de," <https://www.shieldex.de/en/products/shieldex-78-20/>, [Accessed 30-04-2024].